A PRELIMINARY STUDY ON THE EFFECT OF MOTION CORRECTION ON HARDI RECONSTRUCTION

Shireen Elhabian[1], *Yaniv Gur*[1], *Clement Vachet*[1], *Joseph Piven*[2] *for IBIS**, *Martin Styner*[2,3], *Ilana Leppert*[4], *G. Bruce Pike*[4,5], *Guido Gerig*[1]

[1]Scientific Computing and Imaging Institute, Salt Lake City, UT, USA.

[2] Dept. of Psychiatry and [3]Dept. of Computer Science, University of North Carolina, NC, USA.

[4]Dept. of Neurology and Neurosurgery, Montral Neurological Institute, Montral, Quebec, Canada.

[5]Dept. of Radiology, University of Calgary, Calgary, Canada.

ABSTRACT

Post-acquisition motion correction is widely performed in diffusion-weighted imaging (DWI) to guarantee voxel-wise correspondence between DWIs. Whereas this is primarily motivated to save as many scans as possible if corrupted by motion, users do not fully understand the consequences of different types of interpolation schemes on the final analysis. Nonetheless, interpolation might increase the partial volume effect while not preserving the volume of the diffusion profile, whereas excluding poor DWIs may affect the ability to resolve crossing fibers especially with small separation angles. In this paper, we investigate the effect of interpolating diffusion measurements as well as the elimination of bad directions on the reconstructed fiber orientation diffusion functions and on the estimated fiber orientations. We demonstrate such an effect on synthetic and real HARDI datasets. Our experiments demonstrate that the effect of interpolation is more significant with small fibers separation angles where the exclusion of motion-corrupted directions decreases the ability to resolve such crossing fibers.

Index Terms— Diffusion MRI, HARDI, motion correction, interpolation

1. INTRODUCTION

Diffusion-Weighted Imaging (DWI) reveals, in a non-invasive manner, the brain network connectivity by measuring the motion of water molecules in biological tissues. The basic model that enables to infer connectivity maps is Diffusion Tensor Imaging (DTI). Despite its widespread use, it has been shown that DTI is inadequate to capture complex white matter configurations existing in various brain regions. To overcome the limitations of DTI, a different modality known as high angular resolution diffusion imaging (HARDI) [1] has been adopted. In contrast to DTI, HARDI is capable of modeling intra-voxel orientational heterogeneity, such as crossing and merging fiber bundles.

This work is supported by NIH grants ACE RO1 HD 055741 and NA-MIC Roadmap U54 EB005149. *The NIH funded Autism Centers of Excellence Infant Brain Imaging Study (ACE-IBIS) Network: Clinical Sites: University of North Carolina: J. Piven (IBIS Network PI), H.C. Hazlett, C. Chappell; University of Washington: S. Dager, A. Estes, D. Shaw; Washington University: K. Botteron, R. McKinstry, J. Constantino, J. Pruett; Children's Hospital of Philadelphia: R. Schultz, S. Paterson; University of Alberta: L. Zwaigenbaum; Data Coordinating Center: Montreal Neurological Institute: A.C. Evans, D.L. Collins, G.B. Pike, V. Fonov, P. Kostopoulos; Samir Das; Image Processing Core: University of Utah: G. Gerig; University of North Carolina: M. Styner; Statistical Analysis Core: University of North Carolina: H. Gu.

While being inherently a low-resolution and a low-SNR imaging technique, an intrinsic artifact of DWI is its sensitivity to motion [2, 3], which results in a significant signal phase shift, or signal loss [4]. Motion is usually attributed to substantial vibration of the diffusion gradients [5], cardiac pulsation, breathing and head movement comparable to, or larger than the voxel size [6]. This sensitivity is further increased with long acquisition times where subjects are likely to move.

Motion effects can be reduced by real-time motion detection [7, 8], where the acquisition and the source of motion are synchronized, however, this prospective approach for motion correction might affect the acquisition time. A comfortable padding can also be used to minimize subject head motion while urging the participant to remain without movement [9], but this is not always effective in studies involving newborn and infants (e.g. autism diagnosis [10]). Alternatively, the exclusion of one or more gradients bearing strong motion artifacts can be exercised [11], however, this limits the ability to reconstruct crossing fibers especially at small separation angles. As such, post-acquisition motion correction is imperative to guarantee voxel-wise correspondence between different DWIs referring to the same anatomical structure.

A typical motion correction algorithm involves two stages [6]; first, finding the global transformation parameters that would transform all DWIs to the same coordinate frame, then, applying the estimated transformation to the diffusion data. Solving for the transformation parameters usually involves rigidly registering the DWIs to a reference image representing the same anatomical structure, but without being contaminated by motion artifacts, e.g., a non-diffusion weighted image, a T2-weighted image [2], or a model-based reference image for each diffusion weighted image [12].

However, applying the estimated transformation involves reorienting the diffusion gradient vectors [13] to incorporate the rotational component of subject motion, as well as interpolating the DWIs. Nonetheless, such interpolation might increase the partial volume effect [14], while modifying the variance properties of the original images [15]. Further, Euclidean-based interpolation, which is being used by different motion correction algorithms, e.g. FSL-MCFLIRT [16], has been known to not preserve the volume of the diffusion profile [17]. Hence, interpolated diffusion measurements would result in diffusion tensor swelling. This swelling effect might even be more pronounced when dealing with HARDI measurements where higher-order tensors are used to represent orientation distribution functions.

The effect of different interpolation schemes on HARDI-based reconstruction and subsequent analysis seems to have been mostly disregarded by the scientific community. Chao *et al.* [18] investigated such effects on the measurement of fractional anisotropy (FA),

as a result of interpolating diffusion tensor images in spatial normalization for voxel-based statistics. Based on their experimentation on simulated and real data, they concluded that spatial normalization may affect the FA value in brain areas with predominantly crossing fibers. To the best of our knowledge, no quantitative study has been carried out on HARDI-data, although this may have a direct impact on registration, atlas building, tractography, and group differences. Therefore, the outcomes of a HARDI-based study can significantly vary based on the employed interpolation scheme.

In this paper, we use simulated and real data to study the effects of different interpolation schemes, commonly used in motion correction, on reconstructed fiber orientation distribution functions (fODFs), and the detected fiber orientations. Also, we explore the effect of excluding motion-corrupted DWIs, as an alternative to interpolation.

2. METHODS

The effects of motion correction are demonstrated on two datasets; (1) *synthetic data*, where motion (rotation in particular) parameters are known before-hand, and (2) *real data*, where two HARDI acquisitions of the same subject are mixed to mimic noticeable subject motion. In both cases we explore two different approaches for motion correction. In the first approach, motion artifacts are corrected by rotating the corrupted diffusion images, while re-orienting the corresponding gradient directions. This approach involves image interpolation, where various interpolation methods are studied. The re-orientation step was performed using FSL-MCFLIRT [16] with nearest neighbor, trilinear, sinc and spline interpolation techniques. In the second approach, we exclude the affected gradient directions from subsequent computations (i.e., diffusion profile reconstruction).

To study the impact of motion correction on reconstructed diffusion profiles from HARDI scans, we use fiber orientation distribution functions (fODFs). The fODFs were computed using the method proposed by Weldeselassie et al. [19], which models diffusion by estimating symmetric positive definite higher-order tensors. In this work, we only consider fourth-order tensors to avoid the dominant impact of noise on higher orders. The representation of the fODF as a higher-order tensor enables us to extract the fiber orientations by directly applying the tensor decomposition technique proposed by Jiao *et al.* [20].

We use two different measures to quantify the impact of motion correction on the estimated fODFs. In order to quantify the similarity between the original motion-free fODFs and the fODFs corresponding to the motion corrected images, we use the Jensen-Shannon divergence (JSD) which measures similarity between probability distributions, and has been used to quantify differences between ODFs in various studies [21, 22]. Given two probability distributions P and Q, the JSD metric is defined as follows:

$$\mathrm{JSD(P\|Q)} = \frac{1}{2}\left[D_{\mathrm{KL}}(P\|M) + D_{\mathrm{KL}}(Q\|M)\right], \qquad (1)$$

where $M = (P+Q)/2$ and D_{KL} is the Kullback-Leibler divergence. In our case, P and Q are represented as discrete distributions, therefore, the KL divergence takes the following form: $D_{\mathrm{KL}}(P\|Q) = \sum_i P_i \log \frac{P_i}{Q_i}$, where i is the discrete sample index. Note that in order to use the JSD, the fODFs need to be normalized to sum up to 1.

Deviations in fiber orientations due to motion correction may lead to erroneous fiber tracts, therefore, it is important to study this effect by directly comparing the original fiber orientations to the post-correction ones. To that end, we use the mean angular deviation measure defined as follows:

$$\theta^k_{i,j} = \frac{180}{\pi}\left|\cos^{-1}(v^k_i.v^k_j)\right|, \quad \theta = \frac{1}{N}\sum_{k=1}^{N}\theta^k_{i,j}, \qquad (2)$$

where k is the number of fibers compared, and v^k_i and v^k_j correspond to the orientations of fiber k, with and without motion correction. In the simulated data case, we restrict ourselves to two fibers, therefore, $N = 2$ in every voxel. Since any image transformation will not preserve the original fiber orientations ordering, in each comparison we match the two closest fibers, such that $\theta^1 = \min\{\theta^1_{1,1}, \theta^1_{1,2}\}$, and then we compute θ^2 for the remaining pair of fibers. Note that while in the simulated data case we use the mean deviation, in the real data case we use the angular deviation between each pair of fibers, separately (that is, θ^1 and θ^2).

3. EXPERIMENTS

3.1. Synthetic Data

A synthetic, analytical phantom (matrix size 16x16) was created to quantitatively assess interpolation performance and the amount of artifacts it produces. The phantom was generated based on two crossing fiber bundles with a controllable separation angle. This design enables us to rotate the phantom before simulating the diffusion signal in order to mimic the rotational component of the subject motion.

The diffusion signal is generated by simulating two crossing fiber bundles with separation angle $\theta \in \{45^o, 60^o, 75^o, 90^o\}$ using the multi-tensor model as in [23]. Based on typical diffusivities found in the human brain [24], we assume a prolate tensor model with eigenvalues $\lambda_1 = 1.7 \times 10^{-3}$ mm^2/s and $\lambda_2 = \lambda_3 = 0.3 \times 10^{-3}$ mm^2/s. We used the HARDI-like sampling scheme of ISBI-2013 HARDI reconstruction challenge with 64 gradient directions and b-value = 3000 s/mm^2.

To simulate motion, we adopt the random subject motion model in [13], where we studied three different cases with 30%, 50% and 70% of the gradient directions were corrupted by rotating the two-fibers phantom about the z-axis. The rotation angle α was randomly drawn from a normal distribution with zero mean and std of 5^o.

Fig. 1 shows the quantitative comparison between the reconstructed fODFs and the estimated fiber orientations from interpolated diffusion measurements versus the ground truth reconstructions (where there is no motion corruption). One can observe that the effect of interpolation on the fODFs, and on the detected fiber orientations, becomes significant as the percentage of corrupted gradients increases. The JSD is maximal in single fiber voxels indicating that the reconstructed fODFs from interpolated diffusion measurements show increase in the diffusion volume. Furthermore, the effect of interpolation on the fODFs increases for small fiber separation angles. Although excluding corrupted gradient might seem an alternative choice for motion correction, the fiber orientation deviation increases for small fiber separation angles, especially when the percentage of directions being corrupted is increased, a situation which is encountered in studies including newborn and infants.

3.2. Real Data

One healthy subject was scanned twice with a 3.0T Siemens Magnetom TrioTim scanner where Eddy current was compensated for using the Twice-refocused Spine Echo sequence. To simulate noticeable motion, the subject was allowed to move (rotation of about 10^o) between the two scans. DWI datasets were acquired with FOV $= 20 \times 20$ cm, slice thickness $= 2.0$ mm, matrix size $= 106 \times 106$ with 76 axial slices. The diffusion data consisted of one baseline image with zero b-value and 64 DW-images with b-value = 2000 s/mm^2.

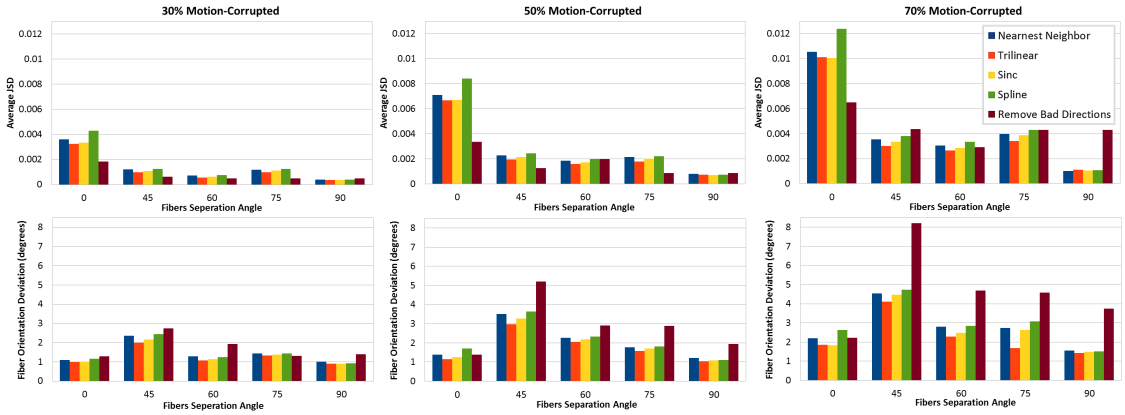

Fig. 1. Simulated data results. Top: The average Jensen-Shannon divergence (JSD) values. Bottom: The average fiber orientation deviation (in degrees). Both metrics are shown as functions of the fibers' separation angles (where 0 indicates a single fiber), and the motion-correction method.

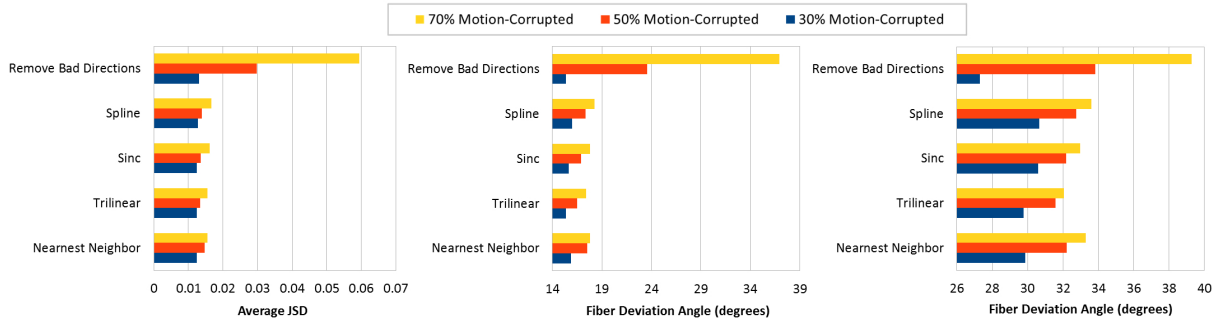

Fig. 2. Real data results. Comparisons of fODFs and the estimated fiber orientations from interpolated diffusion measurements and motion-free data. Left: The average Jensen-Shannon divergence (JSD). Middle: The average fiber orientation deviation of the first detected fiber having the largest volume fraction. Right: average fiber orientation deviation of the second detected fiber having the second largest volume fraction. Those measures are shown as functions of the motion-correction scheme (removing directions versus different interpolation schemes), and different percentages of motion-corrupted directions.

We arbitrarily considered the first out of the two acquisitions as the uncorrupted (w/o motion), and used it as a reference for performance evaluation of different interpolating schemes. A random percentage of DW images (30, 50 and 70%) drawn from the second scan were mixed with the first scan to construct three motion-corrupted datasets. FSL-MCFLIRT [16] was then used to provide the rigid transformation matrix (six degrees of freedom) for each image volume having the baseline image as the reference for motion correction. The gradient directions for each of the three datasets were re-oriented accordingly.

Fig. 2 summarizes the results for the real data case where the effect of interpolation increases with the increase of subject motion, regardless of the interpolation scheme employed. These results were obtained by averaging over voxels within a white matter mask in three consecutive axial slices. Being consistent with the results from our simulations, removing bad direction affects the reconstructed fODFs, as well as the estimated fiber orientations. Sample coronal and axial slices are shown in Fig.3, where one can observe the effect of excluding corrupted directions versus correction via interpolation. The results presented in this figure confirm our observation from the simulated phantom experiment, where less deviation in orientations due to correction are seen in single fiber voxels, such as in the corpus callosum, whereas in regions containing crossing fibers, such as in the centrum semiovale, there are clearly larger deviations. This is especially pronounced when the employed correction scheme was elimination of directions.

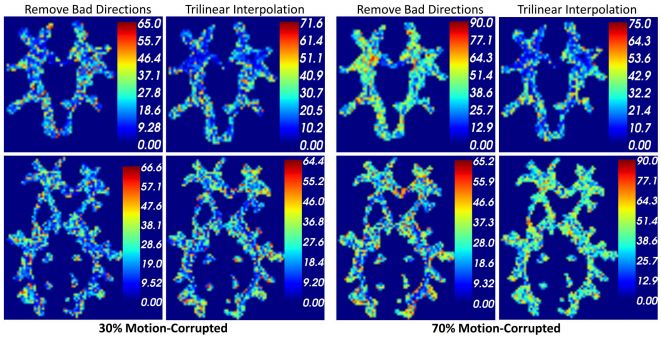

Fig. 3. The average fiber orientation deviation (in degrees) for sample coronal (top) and axial (bottom) slices.

4. CONCLUSION

Although prospective motion correction can be used to reduce motion artifacts in diffusion weighted imaging, this might affect acquisition times. Therefore, post-acquisition motion correction is needed to guarantee voxel-wise correspondences. In this paper, we investigated the effect of various techniques typically employed in correcting for subject motion on subsequent reconstructions. In particular, we showed that image interpolation, as well as removing corrupted directions inevitably affected the reconstructed fiber orientation distribution functions and the detected fiber orientations. Based on simulated phantom of two crossing fibers, and in vivo HARDI dataset, we demonstrated that the effect of interpolation increases with the amount of gradient directions being distorted by subject motion. Using the simulated phantom, we showed that as the fiber separation angle gets smaller the impact of motion correction on the reconstructed fODFs and fiber orientations becomes more pronounced. Furthermore, we showed that the exclusion of gradients bearing strong motion artifacts affects the ability to resolve fiber crossings, especially as the fibers separation angle decreases. Although image interpolation introduces less distortion to the subsequent reconstruction compared to gradients elimination, even in highly motion-corrupted datasets, yet the question on how this deviation would affect subsequent tasks, such as tractography and group analysis, remains open.

5. REFERENCES

[1] David S Tuch, Timothy G Reese, Mette R Wiegell, Nikos Makris, John W Belliveau, and Van J Wedeen, "High angular resolution diffusion imaging reveals intravoxel white matter fiber heterogeneity," *Magnetic Resonance in Medicine*, vol. 48, no. 4, pp. 577–582, 2002.

[2] GK Rohde, AS Barnett, PJ Basser, S Marenco, and C Pierpaoli, "Comprehensive approach for correction of motion and distortion in diffusion-weighted mri," *Magnetic Resonance in Medicine*, vol. 51, no. 1, pp. 103–114, 2004.

[3] Siawoosh Mohammadi, Harald E Möller, Harald Kugel, Dirk K Müller, and Michael Deppe, "Correcting eddy current and motion effects by affine whole-brain registrations: Evaluation of three-dimensional distortions and comparison with slicewise correction," *Magnetic Resonance in Medicine*, vol. 64, no. 4, pp. 1047–1056, 2010.

[4] Jacques-Donald Tournier, Susumu Mori, and Alexander Leemans, "Diffusion tensor imaging and beyond," *Magnetic Resonance in Medicine*, vol. 65, no. 6, pp. 1532–1556, 2011.

[5] Jaana Hiltunen, Riitta Hari, Veikko Jousmäki, Kiti Müller, Raimo Sepponen, and Raimo Joensuu, "Quantification of mechanical vibration during diffusion tensor imaging at 3 t," *Neuroimage*, vol. 32, no. 1, pp. 93–103, 2006.

[6] Ken E Sakaie and Mark J Lowe, "Quantitative assessment of motion correction for high angular resolution diffusion imaging," *Magnetic resonance imaging*, vol. 28, no. 2, pp. 290–296, 2010.

[7] Emmanuel Caruyer, Iman Aganj, Christophe Lenglet, Guillermo Sapiro, and Rachid Deriche, "Motion detection in diffusion mri via online odf estimation," *International journal of biomedical imaging*, vol. 2013, 2013.

[8] Tobias Kober, Rolf Gruetter, and Gunnar Krueger, "Prospective and retrospective motion correction in diffusion magnetic resonance imaging of the human brain," *Neuroimage*, vol. 59, no. 1, pp. 389–398, 2012.

[9] José M Soares, Paulo Marques, Victor Alves, and Nuno Sousa, "A hitchhiker's guide to diffusion tensor imaging," *Frontiers in neuroscience*, vol. 7, 2013.

[10] Andrew L Alexander, Jee Eun Lee, Mariana Lazar, Rebecca Boudos, Molly B DuBray, Terrence R Oakes, Judith N Miller, Jeffrey Lu, Eun-Kee Jeong, William M McMahon, et al., "Diffusion tensor imaging of the corpus callosum in autism," *Neuroimage*, vol. 34, no. 1, pp. 61–73, 2007.

[11] Zhexing Liu, Yi Wang, Guido Gerig, Sylvain Gouttard, Ran Tao, Thomas Fletcher, and Martin Styner, "Quality control of diffusion weighted images," in *SPIE Medical Imaging*. International Society for Optics and Photonics, 2010, pp. 76280J–76280J.

[12] Yu Bai and Daniel C Alexander, "Model-based registration to correct for motion between acquisitions in diffusion mr imaging," in *Biomedical Imaging: From Nano to Macro, 2008. ISBI 2008. 5th IEEE International Symposium on*. IEEE, 2008, pp. 947–950.

[13] Alexander Leemans and Derek K Jones, "The b-matrix must be rotated when correcting for subject motion in dti data," *Magnetic Resonance in Medicine*, vol. 61, no. 6, pp. 1336–1349, 2009.

[14] Adolf Pfefferbaum, Edith V Sullivan, Maj Hedehus, Kelvin O Lim, Elfar Adalsteinsson, and Michael Moseley, "Age-related decline in brain white matter anisotropy measured with spatially corrected echo-planar diffusion tensor imaging," *Magnetic resonance in medicine*, vol. 44, no. 2, pp. 259–268, 2000.

[15] Gustavo K Rohde, Alan S Barnett, Peter J Basser, and Carlo Pierpaoli, "Estimating intensity variance due to noise in registered images: applications to diffusion tensor mri," *Neuroimage*, vol. 26, no. 3, pp. 673–684, 2005.

[16] Mark Jenkinson, Peter Bannister, Michael Brady, and Stephen Smith, "Improved optimization for the robust and accurate linear registration and motion correction of brain images," *Neuroimage*, vol. 17, no. 2, pp. 825–841, 2002.

[17] Ofer Pasternak, Nir Sochen, and Peter J Basser, "Metric selection and diffusion tensor swelling," in *New Developments in the Visualization and Processing of Tensor Fields*, pp. 323–336. Springer, 2012.

[18] Tzu-Cheng Chao, Ming-Chung Chou, Pinchen Yang, Hsiao-Wen Chung, and Ming-Ting Wu, "Effects of interpolation methods in spatial normalization of diffusion tensor imaging data on group comparison of fractional anisotropy," *Magnetic resonance imaging*, vol. 27, no. 5, pp. 681–690, 2009.

[19] Yonas T Weldeselassie, Angelos Barmpoutis, and M Stella Atkins, "Symmetric positive semi-definite cartesian tensor fiber orientation distributions (ct-fod)," *Medical Image Analysis*, 2012.

[20] Fangxiang Jiao, Yaniv Gur, Chris R Johnson, and Sarang Joshi, "Detection of crossing white matter fibers with high-order tensors and rank-k decompositions," in *Information Processing in Medical Imaging*. Springer, 2011, pp. 538–549.

[21] Ming-Chang Chiang, Marina Barysheva, Agatha D Lee, Sarah Madsen, Andrea D Klunder, Arthur W Toga, Katie L McMahon, Greig I De Zubicaray, Matthew Meredith, Margaret J Wright, et al., "Brain fiber architecture, genetics, and intelligence: a high angular resolution diffusion imaging (hardi) study," in *Medical Image Computing and Computer-Assisted Intervention–MICCAI 2008*, pp. 1060–1067. Springer, 2008.

[22] Julien Cohen-Adad, Maxime Descoteaux, and Lawrence L Wald, "Quality assessment of high angular resolution diffusion imaging data using bootstrap on q-ball reconstruction," *Journal of Magnetic Resonance Imaging*, vol. 33, no. 5, pp. 1194–1208, 2011.

[23] David S Tuch, "Q-ball imaging," *Magnetic Resonance in Medicine*, vol. 52, no. 6, pp. 1358–1372, 2004.

[24] Erick Jorge Canales-Rodríguez, Lester Melie-García, and Yasser Iturria-Medina, "Mathematical description of q-space in spherical coordinates: Exact q-ball imaging," *Magnetic Resonance in Medicine*, vol. 61, no. 6, pp. 1350–1367, 2009.